SUPPLEMENTARY INFORMATION

Insights into dynein motor domain function from a 3.3 Å crystal structure

Helgo Schmidt, Emma S. Gleave, Andrew P. Carter

MRC Laboratory of Molecular Biology Hills Road, Cambridge, CB2 0QH, UK

Correspondence should be addressed to A.P.C. (cartera@mrc-lmb.cam.ac.uk)

Supplementary Figures

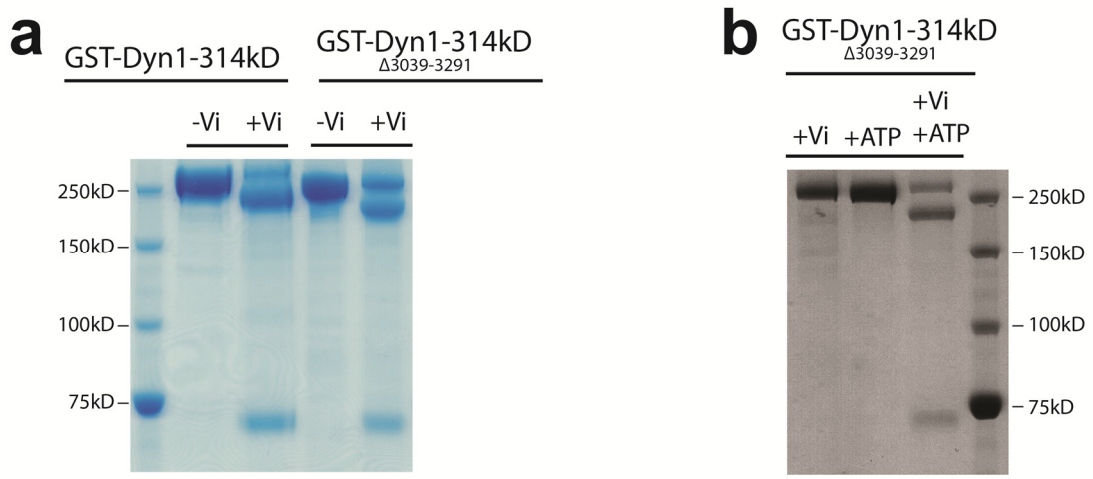

Supplementary Figure 1 The crystallization construct is able to undergo ATP.vanadate mediated UV cleavage at AAA1. (**a**) The crystallization construct (GST-Dyn1-314kD$_{\Delta 3039\text{-}3291}$) and a related construct with a full length stalk (GST-Dyn1-314kD) were incubated with ATP in the absence (-Vi) or presence of (+Vi) of vanadate followed by UV-irradiation. The presence of vanadate causes cleavage of the protein in AAA1 leading to the appearance of a ≈ 70kD fragment for both constructs. (**b**) ATP-dependence of the cleavage reaction. GST-Dyn1314kD$_{\Delta 3039\text{-}3291}$ was incubated with vanadate (+Vi), with ATP (+ATP) or in the presence of both compounds (+ATP, +Vi). Cleavage only occurs in the presence of ATP and vanadate.

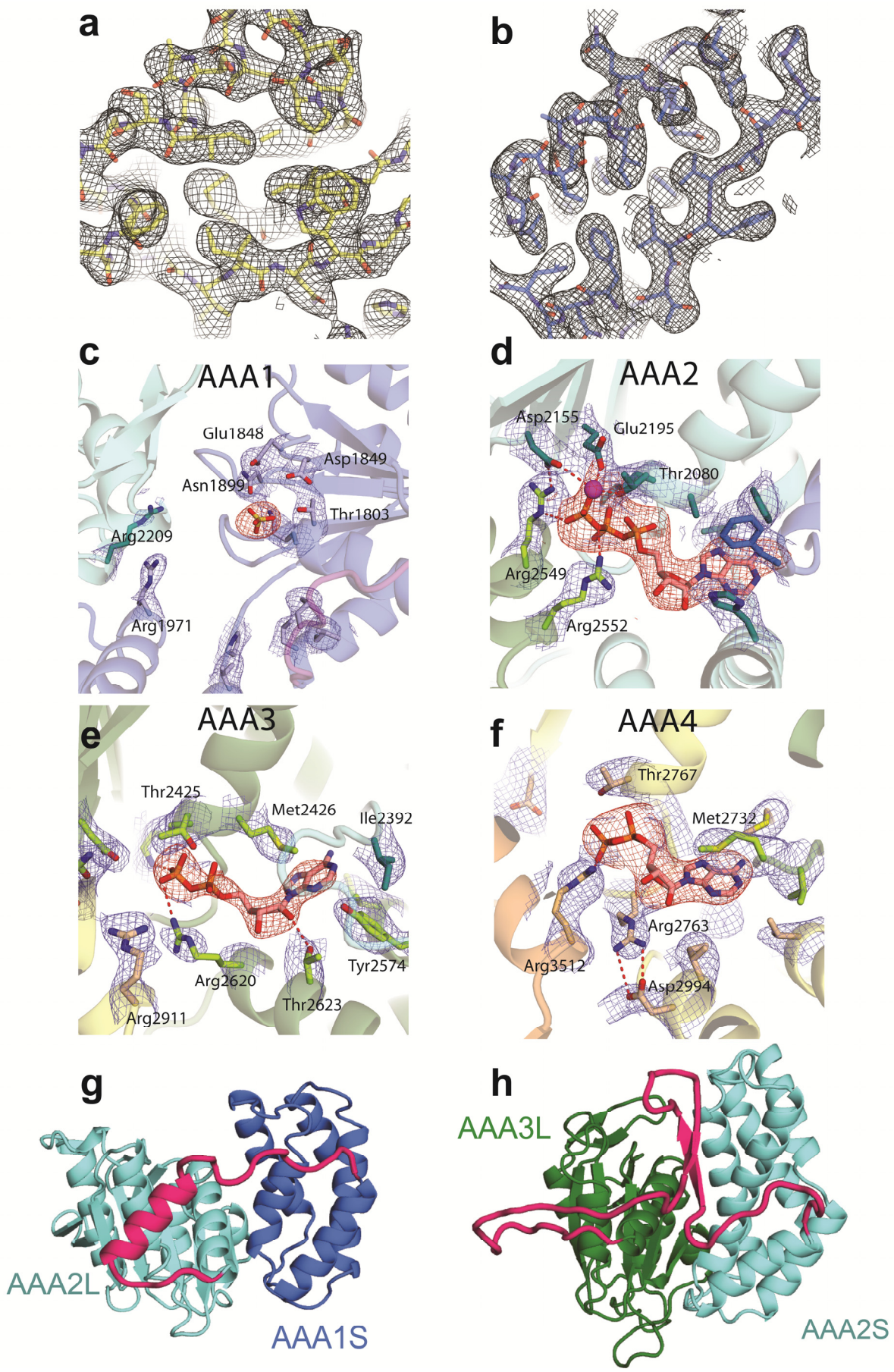
a
b
c
AAA1
Glu1848
Asp1849
Asn1899
Thr1803
Arg2209
Arg1971
d
AAA2
Asp2155
Glu2195
Thr2080
Arg2549
Arg2552
e
AAA3
Thr2425
Met2426
Ile2392
Tyr2574
Arg2620
Thr2623
Arg2911
f
AAA4
Thr2767
Met2732
Arg2763
Arg3512
Asp2994
g
AAA2L
AAA1S
h
AAA3L
AAA2S

Supplementary Figure 2 Examples of the electron density quality in different AAA+ domains and connector peptides between AAA+ domains. Panels (**a**) and (**b**) refer to the overall quality of the electron density in (**a**) AAA4 and (**b**) AAA1 (ATP soaked crystal structure). Panels (**c**- **f**) refer to the quality of the electron density in the nucleotide binding sites of AAA+ domains AAA1 – AAA4: (**c**) AAA1 site (ATP-soaked crystal-structure), (**d**) AAA2 site (LuAc-1 derivative), (**e**) AAA3 site (ATP-soaked crystal-structure) and (**f**) AAA4 site (ADP-soaked crystal-structure). Selected amino-acid residues are labelled. In all panels, the map-sharpened 2Fo-Fc electron density is shown as mesh in grey or lightblue and contoured at 1σ. The map-sharpened Fo-Fc difference density for the ligands occupying the nucleotide bindings sites (sulphate ion in the case of AAA1) is shown as mesh in red and contoured at 3σ. (**g**) connector peptide (magenta) between AAA1S and AAA2L. (**h**) connector peptide (magenta) between AAA2S and AAA3L.

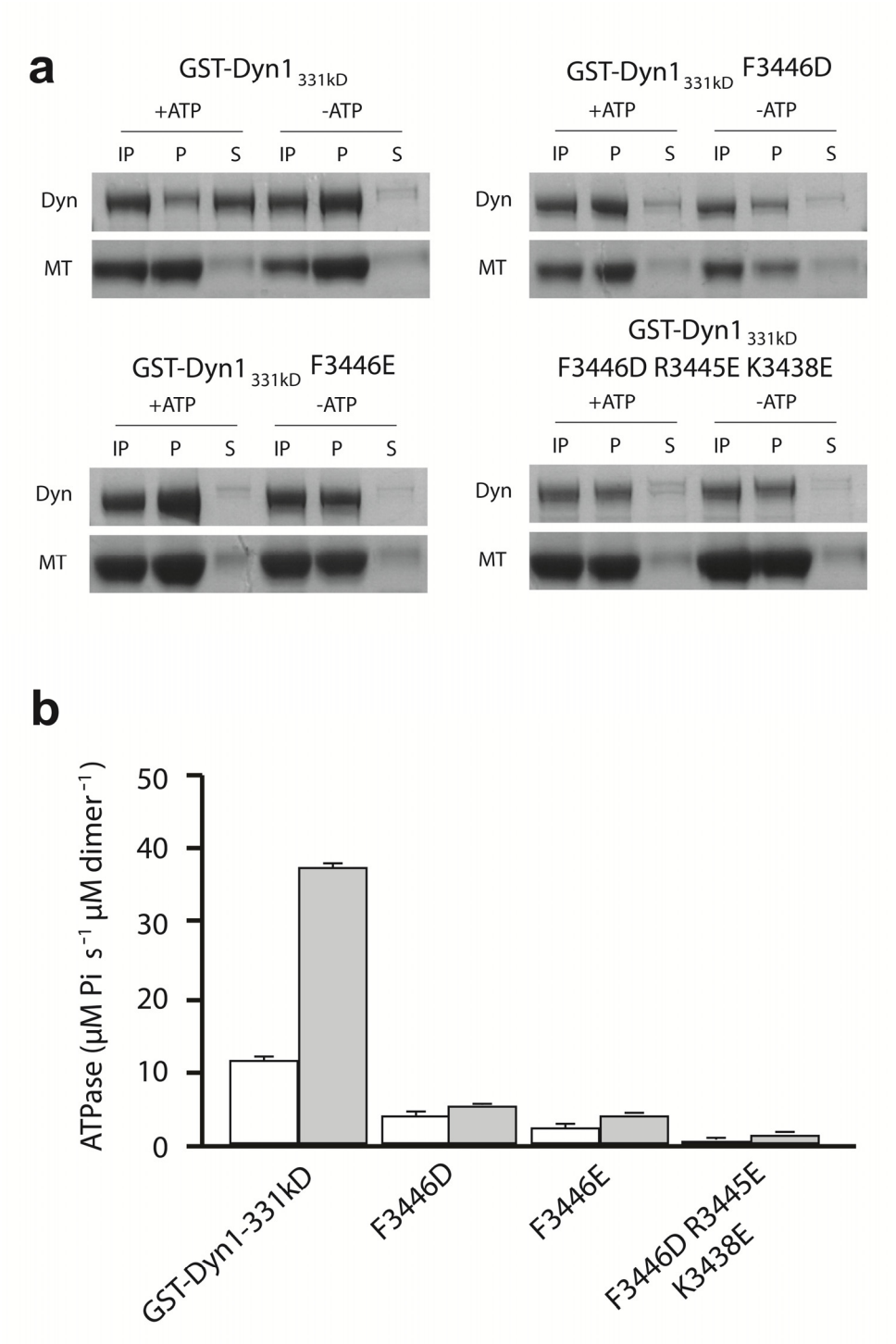

Supplementary Figure 3 Microtubule cosedimentation and ATPase assays. (**a**) Wild-type (GST-$_{Dyn1331kD}$) and variants with a mutated AAA5-linker interface were incubated with microtubules in the presence and absence of ATP. The samples were centrifuged and subsequently analysed by SDS-PAGE. Disrupting the docking site between AAA5 and the linker interferes with ATP mediated release from

microtubules. IP = input, P = pellet and S = supernatant. (**b**) The basal (white) and MT-stimulated (shaded) ATPase activities of the wild-type (GST-Dyn1$_{331kD}$) dynein motor domain and variants with a mutated AAA5-linker interface. Disrupting the docking site between AAA5 and the linker leads to significantly reduced ATPase activities and prevents microtubule mediated stimulation of the ATPase activity. All measurements were carried out in duplicate and the error bars represent the s.d..

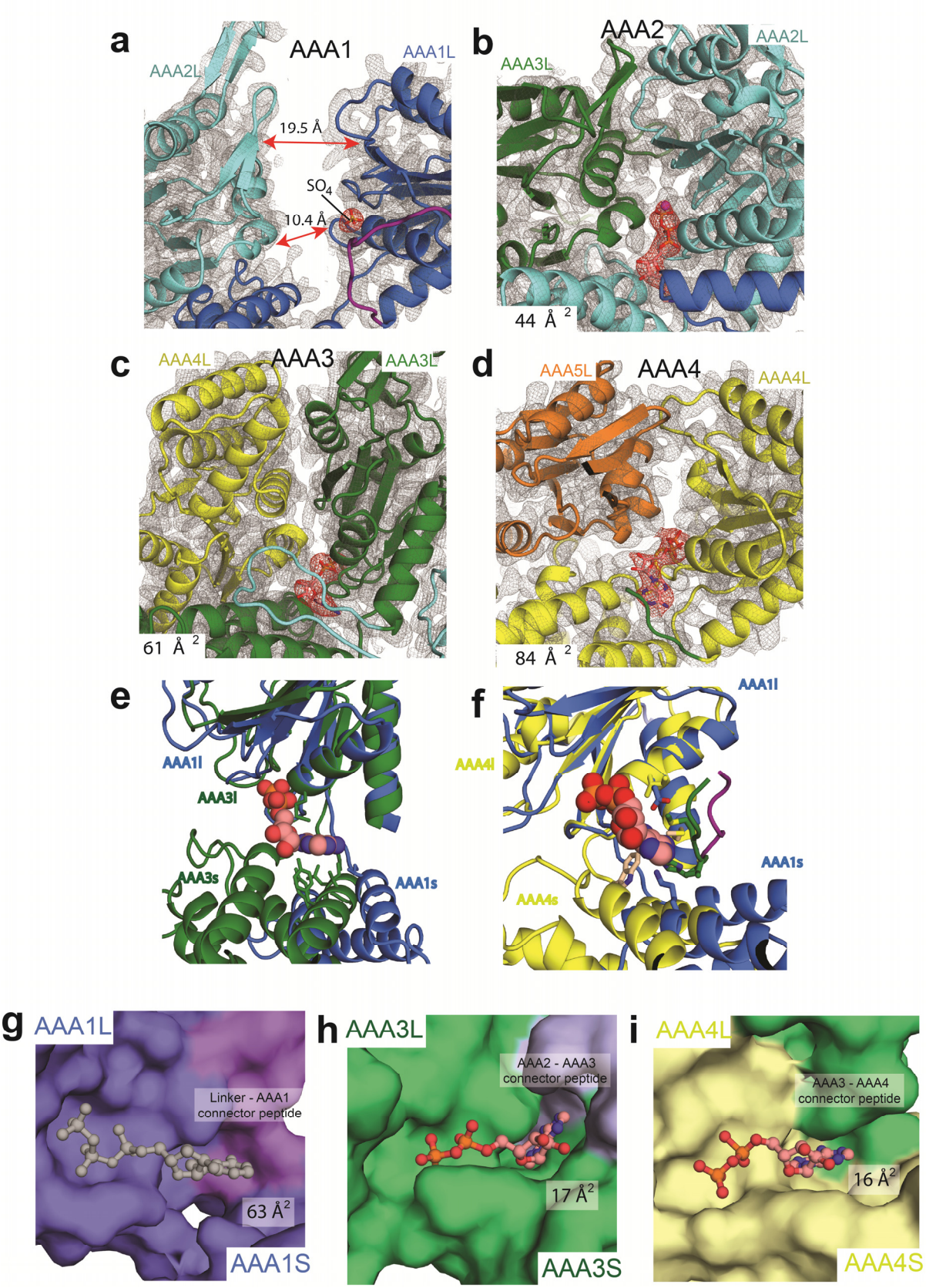
a
AAA1
AAA2L
AAA1L
19.5 Å
SO4
10.4 Å
b
AAA2
AAA2L
AAA3L
44 Å 2
c
AAA4L
AAA3
AAA3L
61 Å 2
d
AAA5L
AAA4
AAA4L
84 Å 2
e
AAA1l
AAA3l
AAA3s
AAA1s
f
AAA1l
AAA4l
AAA1s
AAA4s
g
AAA1L
Linker - AAA1
connector peptide
63 Å2
AAA1S
h
AAA3L
AAA2 - AAA3
connector peptide
17 Å2
AAA3S
i
AAA4L
AAA3 - AAA4
connector peptide
16 Å2
AAA4S

Supplementary Figure 4 Nucleotide binding to sites AAA1-AAA4. (**a-d**) Different degrees of cleft closure in nucleotide binding sites AAA1-AAA4. (**a**) Open cleft of AAA1 in the ADP-soaked crystal structure. A sulfate-ion binds to the Walker A motif. (**b**) Closed cleft in AAA2 in the LuAc-1 derivative crystal structure. (**c**) Semi-closed cleft of AAA3 and (**d**) semi-closed cleft of AAA4 (both ADP-soaked crystal structure). The solvent accessible area of the nucleotides in AAA2-AAA4 is written in bottom right corner of each respective panel. The map-sharpened 2Fo-Fc difference density is shown in grey and contoured at 1σ and the Fo-Fc difference density around the nucleotides is shown in red and contoured at 3σ throughout the appropriate panels. (**e**) The P-loops of AAA1 and AAA3 are aligned and residues within a 4 Å radius from the nucleotide base are shown in stick representation. In AAA3, hydrophobic residues of the large and small domains form a binding pocket for the nucleotide base. In contrast, in AAA1 the large and small domains have swung open leading to much fewer residues that have the potential to contact the nucleotide base. (**f**) Alignment as described in (e) with AAA1 and AAA4. Compared to AAA1, there are more hydrophobic residues in AAA4 that can contribute to nucleotide base binding. (**g-i**) Comparison of the base binding pockets of AAA1, AAA3, AAA4. (**g**) Open pocket of the AAA1 nucleotide binding site harbouring a modelled ATP-molecule (grey) (ADP-soaked crystal structure). (**h**) Closed pockets of the AAA3 and (**i**) AAA4 nucleotide binding sites (ADP soaked crystal structure). The accessible surface area of the adenine base in (g-i) is indicated in $Å^2$ and shows that a base modelled into AAA1 is more accessible than those observed in AAA3 and AAA4.

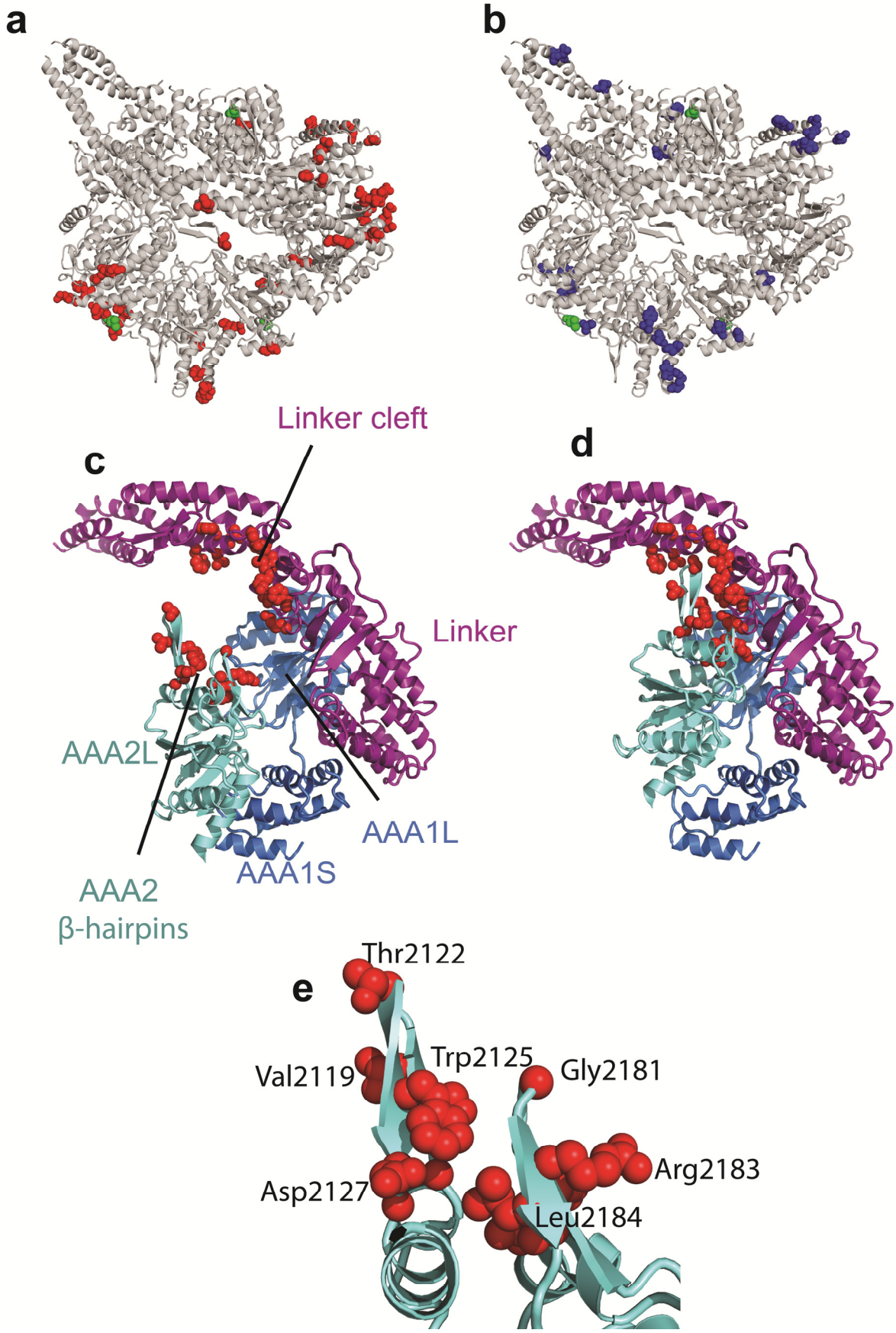
a
b
Linker cleft
c
d
Linker
AAA2L
AAA1L
AAA1S
AAA2
β-hairpins
e
Thr2122
Trp2125
Val2119
Gly2181
Arg2183
Asp2127
Leu2184

Supplementary Figure 5 Crystallographic environment of the dynein motor domain and simulated closure of the AAA1 nucleotide binding site. (**a**) and (**b**) different crystallographic environments for the two protein copies in the asymmetric unit. The dynein motor domain is depicted as grey cartoon representation. (**a**) Molecule A and (**b**) Molecule B. Amino-acid residues involved in crystal packing contacts ($\leq$ 3.5 Å) are highlighted as spheres. red = contacts specific for Molecule A, blue = contacts specific for Molecule B, green = contacts common to both molecules. Only a few contact sites are common to both molecules, the majority of crystal contacts is either specific for molecule A or molecule B. (**c**) and (**d**) simulated closure of the cleft between AAA1 and AAA2 based on the ATP-bound crystal structure of the AAA+ family member NtrC. For clarity, only the linker, AAA1 and the AAA2L domains are shown in color-coded cartoon representation. Conserved amino-acid residues are highlighted as red spheres. (**c**) Situation as observed in the crystal structure presented here. The conserved patches on the AAA2 β-hairpins and the linker cleft are approximately 18 Å away from each other. (**d**) The modelled closure of the AAA1 site would bring both regions in close contact. (**e**) Close up of the AAA2 β-hairpin inserts. Conserved amino-acid residues are represented as red spheres and labelled.